Effect of as-deposited residual stress on transition temperatures of VO_2 thin films

Kuang Yue Tsai and Tsung-Shune Chin[a)]
Department of Materials Science and Engineering, National Tsing Hua University, Hsinchu 30043, Taiwan

Han-Ping D. Shieh
Institute of Electro-Optical Engineering, National Chiao-Tung University, Hsinchu 30010, Taiwan

Cheng Hsin Ma
Materials Science and Engineering, and Frederick Seitz Materials Research Laboratory, University of Illinois at Urbana-Champaign, Urbana, Illinois 61801

(Received 13 October 2003; accepted 12 April 2004)

Transmittance loops upon thermal cycling of VO_2 thin films were found to change among films with different fabrication conditions that lead to different transition temperatures (Tts) from that of a strain-free VO_2 single crystal, 68 °C. The residual stresses in the films quantitatively determined from x-ray diffractometry were used to explain this variation. Electron spectroscopy for chemical analysis spectra showed that the difference in the binding energy of core electrons $2p_{1/2}$ and $2p_{3/2}$ of the vanadium atom are affected by residual stress and proportional to Tts of the films. The bond length between vanadium and oxygen atoms at room temperature varies with different residual stresses and, furthermore, affects the movements of both atoms during phase change (and hence the Tt of VO_2 thin films). Residual stresses also affect the hysteresis span of the transmittance loop. The relationship between the residual stress of as-deposited VO_2 films and the relative positions between vanadium and oxygen atoms are also delineated in detail.

I. INTRODUCTION

VO_2 with a rutile structure is a well known thermochromic material with a reported reversible phase transition around 68 °C,[1,2] especially for a bulky single-crystalline one. At high temperatures, its structure is tetragonal; while at low temperatures, its structure is monoclinic.[1,2] This reversible phase transition exhibits high cycleability because it is associated only with local movement of atoms, consequently leading to great changes in optical and electrical properties. The literature shows a fourth order change in resistivity and a substantial change in transmittance within the IR region during the phase change of single-crystal rutile VO_2. Reversible changes enable VO_2 devices as electrical or thermochromic switches.

Several approaches to deposit rutile VO_2 films have been reported, such as sputter deposition,[3–5] evaporation,[6,7] pulse laser deposition,[8] and sol-gel coating.[9–12] With different deposition processes, optical-switching performances of VO_2 films are also different. Here we define the transition temperature (Tt) as the midpoint of the change in transmittance during heating. The Tts of un-doped VO_2 were reported with values scattered among authors by different investigations; and they were 18 °C[15], 51 °C,[3] 62 °C,[13] 73 °C,[2] and 78 °C,[14] respectively. The hysteresis width of each transmittance–temperature curve was also different. Regardless of measurement methods, the variations in the Tts had been suggested to arise from the inhomogeneity and strained structure.[16]

Larry A. Ladd and William Paul[17] reported the relationship between external stress and Tt. They claimed that the compressive stress along c-axis of VO_2 single crystal reduces the Tt and the stress exerted along a- or b-axis spans the hysteresis width. A large variation of Tt in epitaxial VO_2 was attributed to the contraction or expansion of c-axis.[15] For a polycrystalline film there are many factors that modify the Tt of VO_2 thin film, such as the structure and residual stress of the thin film. The main factors affecting the final stress states of thin films are intrinsic stress and thermal stress. The intrinsic stress, correlated with the microstructures of films such as morphology, texture, and grain size, usually includes the tensile stress formed during the coalescences of the island

[a)]Address all correspondence to this author.
e-mail: tschin@mx.nthu.edu.tw
DOI: 10.1557/JMR.2004.0299

structures and the compressive stress arising from defects, vacancies, and impurities. After film processing, the cooling procedure results in thermal stress due to the difference in thermal expansion coefficients of the film and the substrate. The thermal stress σ_{th} can be derived from Hook's law as

$$\sigma_{th} = \left(\frac{E_f}{1-\nu_f}\right)\epsilon = \left(\frac{E_f}{1-\nu_f}\right)(\alpha_s - \alpha_f)(T_r - T_s) \quad , \quad (1)$$

where E_f and υ_f are Young's modulus and Poisson's ratio of the film, respectively; α_s and α_f are the thermal expansion coefficients of substrate and film, respectively; while T_r and T_s are room temperature and processing temperature, respectively. The microstructure, such as vacancies or inhomogeneity formed during processing, also changes the effective thermal stress exerted on thin films by some mechanisms (such as movement of dislocations) because the distributions of local yield stress or strain in the polycrystalline film are not uniform.

As the thickness of as-deposited film decreases, the effect of residual stress on crystalline structure becomes more significant on the electric, optical, and mechanical performances of the film. During phase change, the relative forces among atoms in VO_2 will affect processes of atomic movements so that initial structure of VO_2, under the external residual stresses, is an important issue worthy of investigation. Specifically, by adjusting the residual stress and processing conditions, it is possible to modify the optical-switching property of VO_2 without doping impurities. This study focused on quantitatively understanding the relationship between the residual stress and the optical switching properties such as Tt and hysteresis width of polycrystalline VO_2 films prepared by rf-magnetron sputtering. We also tried to correlate the variations in binding energy of core electrons between vanadium and oxygen, elucidated by ESCA analyses, with the residual stress. Furthermore, a structure model is proposed to describe the variations of Tt under different tensile stress values of VO_2 thin films.

II. EXPERIMENTAL

V_2O_5 targets were prepared by powder compaction and then sintered in air at 650 °C for 30 min and cooled down to room temperature in air. Films were deposited by rf-magnetron sputtering with a target of 2-inches in diameter. The distance between the substrate and the target for sputtering was 10 cm. The vacuum chamber was evacuated to 10^{-5} Torr and then back-filled with a mixture of Ar and oxygen to a certain total gas pressure. Ar and oxygen were pre-mixed in a small chamber at a positive pressure 0.13 to 0.18 MPa before being led into the vacuum chamber to maintain a sputtering pressure 30 or 40 mTorr. The process pressure was measured using a capacitance manometer (MKS Baratron gauge). The substrate temperature (*Ts*) and sputtering power were kept at 400 °C and 90 w, respectively, under an oxygen flow ratio (R_{fo}) of 0.08 to 0.04, where $R_{fo} = (fO_2)/(fO_2 + fAr)$ and f is the flow rate of the gas in sccm. Well-cleaned Corning 7059 glasses were used as substrates, which were heated by irradiation lamps during sputtering. The temperature was measured in-situ by using a thermocouple. ESCA was used to measure the binding energy of core electrons of $V_{2p3/2}$ and O_{1s}.

X-ray diffraction (XRD) patterns were recorded by a diffractometer (D/max-IIB, Rigaku) in the 2θ-range 10–50°. Surface morphology, microstructures, and thickness of films were examined by SEM. The thickness of all films was kept at about 90 nm, as shown in Fig. 1. The light source used to measure the transmittance at different temperatures was a semiconductor laser with a wavelength 1.5 μm.

The residual stress was measured by using a four-circle diffractometer with improved $\sin^2\psi$ method proposed by C.H. Ma et al.[17] As shown in the upper part of Fig. 2, *S*1 and *S*2 are the directions on the sample surface and *S*3 is the normal to the sample surface. *L*3, shown in the lower part of Fig. 2, is the normal of measuring plane (*hkl*) that has an angle α with respect to the sample surface. Through the measurement, the sample was rotated about the *S*1 axis for an angle ψ and the incident angle of x ray was kept at γ degree. The lattice spacing $d_{\alpha\psi}$ was derived from the position of the diffraction peak for the given reflection (*hkl*) and the strain (ϵ) from the residual stress (σ) can be expressed by the equation:

$$\epsilon = \frac{d_{\alpha\psi} - d_0}{d_0} = \frac{1+\nu_f}{E_f}\sigma\cos^2\alpha\sin^2\psi + \frac{1+\nu_f}{E_f}\sigma\sin^2\alpha - \frac{2\nu_f}{E_f}\sigma \quad , \quad (2)$$

where d_0 is the initial lattice spacing when $\psi = 0$. By using Eq. 2, the residual stress σ can be derived from the slope of the linear fitting between the fraction change in lattice spacing and the term $\cos^2\alpha\sin^2\psi$, as shown in Fig. 3. It can be expressed by following equation:

$$\sigma = \frac{E_f}{1+\nu_f}s \quad . \quad (3)$$

The difference between the traditional $\sin^2\psi$ method and this one is an additional geometrical correction factor $\cos^2\alpha$, which uses the grazing incident angle. The residual stress of VO_2 thin film derived from Eq. (3) was based on the assumption that the Poisson's ratio of the film was 0.25 and the Young's modulus of VO_2 films, measured by MTS Nano Indenter XP system, was 100 GPa in all samples.

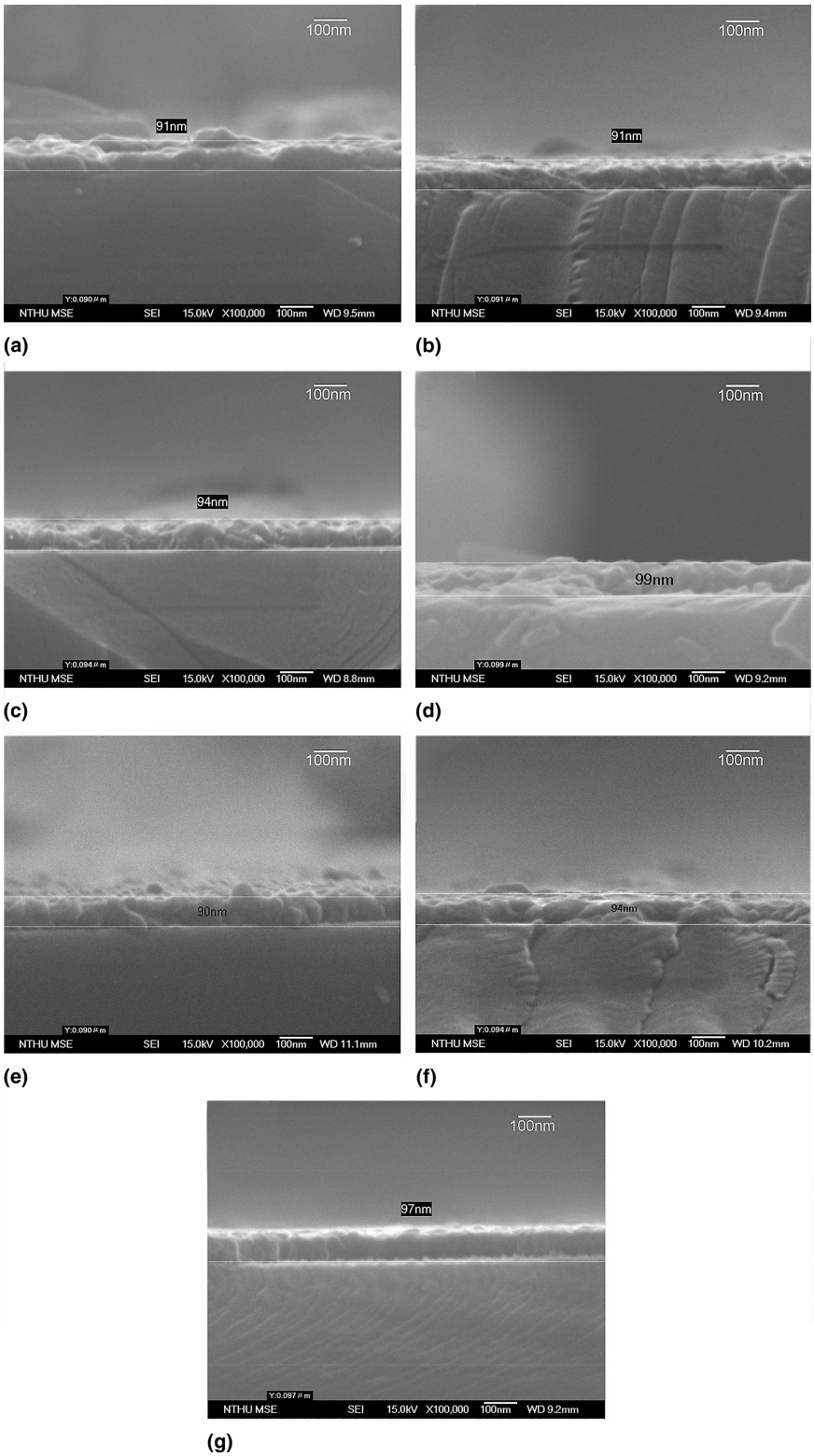

FIG. 1. Thickness measurement by SEM micrographs from film cross-sections.

III. RESULTS

The grain size is proportional to the energy of particles impinging on the substrate at the same substrates temperature. Lower gas pressures in pre-mixed and main chambers profit this situation due to fewer collisions between gas and sputtered-out particles; thus the energy loss is lowered. This fact is manifested from Table I. On the other hand, fewer collisions between gas and

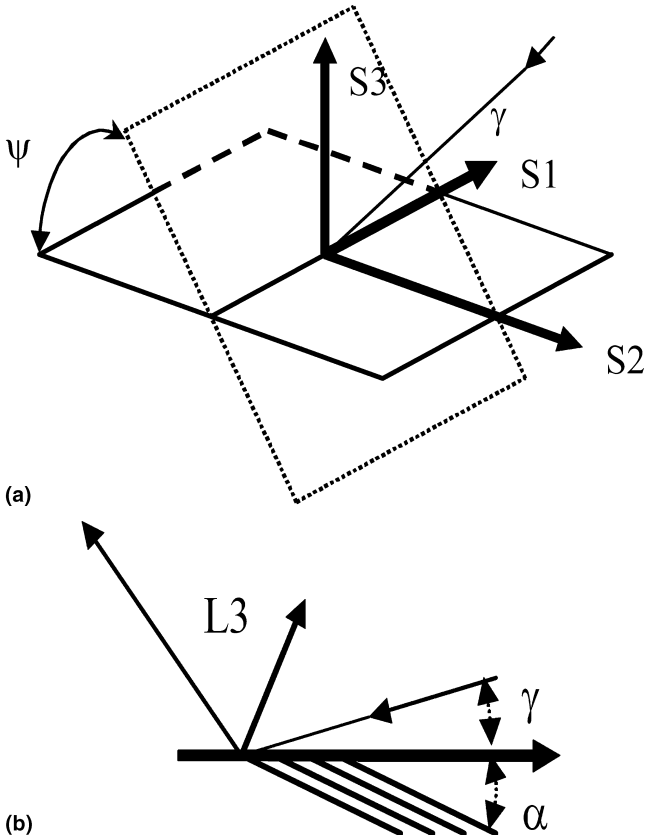

FIG. 2. (a) Definition of the coordinates of the sample and angles ψ and γ, and (b) Incident x-ray and diffraction directions and the angles γ and α.

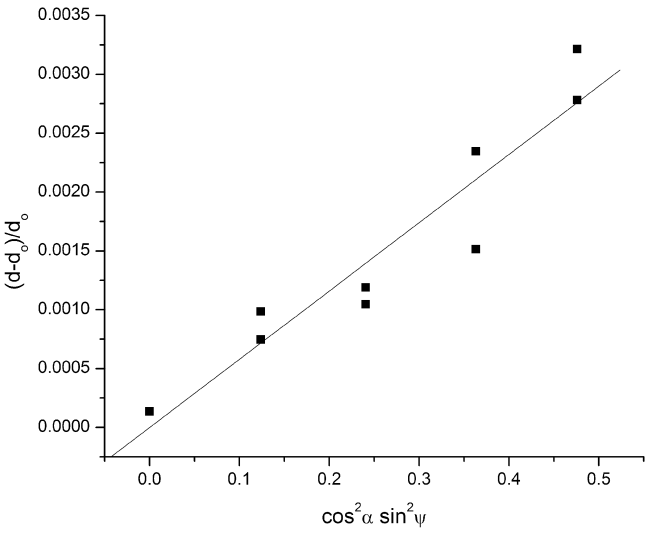

FIG. 3. The plot $(d-d_0)/d_0$ versus $\cos^2\alpha\sin^2\psi$ of sample E.

sputtered-out particles also lower the oxygen content of the thin films, so that higher oxygen partial pressure is also required for the fabrication of VO_2 thin film under lower gas pressures.

TABLE I. Grain size of thin film and gas pressure in pre-mixed chamber and main chamber during thin film fabrication.

Sample name	Average grain size (nm)	$P_{pre\text{-}mixed}$ (MPa)	P_{main} (mTorr)
A	55	0.145	50
B	74	0.182	40
C	88	0.145	40
D	102	0.182	30
E	115	0.131	40
F	118	0.145	30
G	121	0.131	30

Table II summarizes the Tts and hysteresis widths of all studied films. A larger hysteresis width accompanies a higher Tt. Results of ESCA analyses are shown in Table III. The energy differences between core electrons of $V_{2p3/2}$ and O_{1s} are compared with published data[11,12,18,19] to exclude the energy shifting of each apparatus. The relative positions between certain vanadium and oxygen atoms at room temperature affect not only energy levels of the core electrons but also the threshold energy required to move atoms to the equilibrium positions after phase transition. As residual stress increases in the film with smaller grain size, smaller energy differences between measured and typical value imply (for those atoms) the higher similarity of relative positions in measured film respective to typical VO_2 structure. Furthermore, the Tt is also closer to typical value. On the contrary, the residual stress relaxes as grain size grows larger, indicating that the structure of each film is much closer to typical VO_2 so that its energy difference is also closer to the published values. As shown in Fig. 4, as the average grain size becomes larger, the residual stress increases at first. However, when the grain size increases further, the residual stress starts to decay.

As shown in Fig. 5, Tts increases with increasing residual stress from samples A to E. On the other hand, a larger hysteresis width is also accompanied with larger residual stress in the film with a grain size less than 115 nm, as shown in Fig. 6. However, the hysteresis width increases and approaches a constant value as the grain sizes increases, as shown in Fig. 7. Because all the measured Tts of these samples are lower than the typical

TABLE II. Tt and hysteresis width of studied films.

Sample name	Transition temperature (Tt, °C)	Hysteresis width (Hw, °C)
A	45.60	6.8
B	49.93	8.8
C	50.90	9.7
D	51.93	10.1
E	53.98	11.0
F	54.19	11.38
G	54.38	11.09

TABLE III. The difference in binding energies of core electrons O_{1s} and $V_{2P3/2}$ of the studied films and some data in the references.

Sample name	O_{1s}	$V_{2P3/2}$	ΔE	Stress (MPa)
Reference 11	529.8	516.2	13.6	
Reference 12	529.8	516.1	13.7	
Reference 18	529.9	516.2	13.7	
Reference 19	529.9	516.3	13.6	
A	530.0	516.9	13.1	249.6
B	530.0	516.7	13.3	308.8
C	529.8	516.4	13.4	328.8
D	529.9	516.5	13.4	395.2
E	529.9	615.5	13.4	464.0
F	529.9	516.5	13.4	352
G	529.9	516.4	13.5	285.6

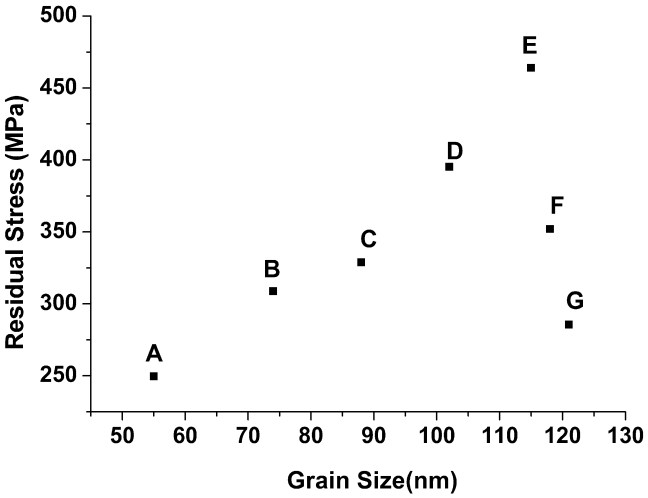

FIG. 4. The relationship between the residual stress and the average grain sizes.

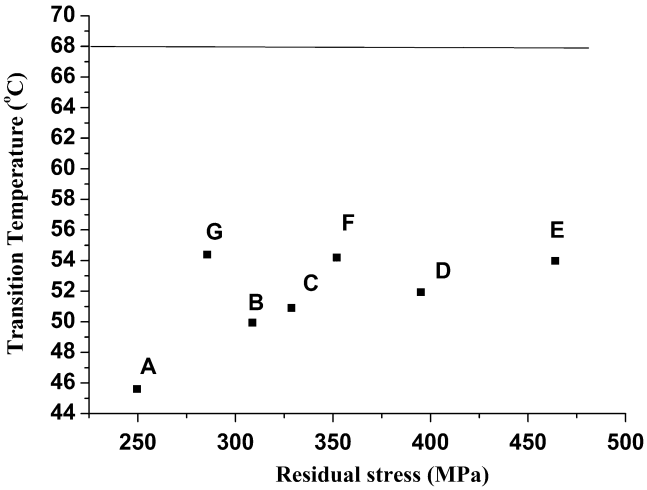

FIG. 5. The relationship between residual stress and Tt of films (the horizontal line being the typical Tt of VO_2).

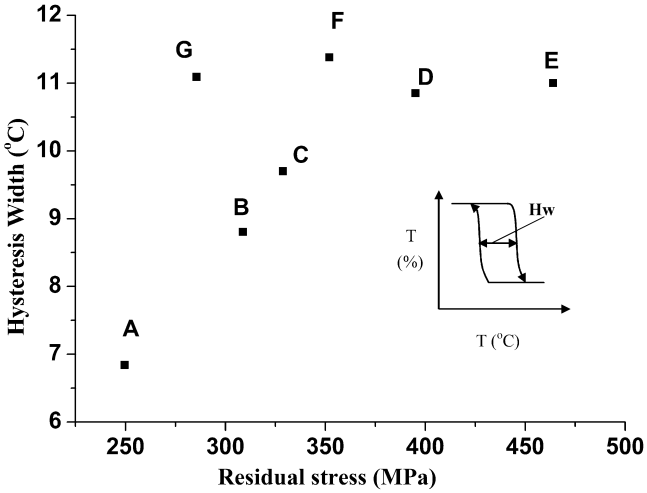

FIG. 6. The relationship between hysteresis width and film stress.

value around 68 °C, contraction of c-axis in all samples is the main reason. The degree of contraction is quite different from sample to sample. This result implies that the residual stress tends to contract c-axis and to distort a- or b- axis. The relationship between the residual stress and the structure is delineated in detail later.

IV. DISCUSSION

Theoretically, the residual stress of sputter-deposited thin films contains intrinsic and external stress. The intrinsic stress is associated with the deposition process and microstructure, while the source of external residual stress is the interaction between the film and the substrate during cooling. To understand how the final measured residual stress is formed, we have to separate stress formation into two steps. The first step includes the formation of film microstructure during different processing conditions. In the second step, during cooling, the microstructures of the films affect the modification caused by interaction between the film and substrate. The grain boundary relaxation model is most often used to explain the formation of intrinsic tensile stress in polycrystalline films in the early stage of film formation.[20,21] During the first step, film grows from isolated randomly oriented grains. As grains grow intact, the boundaries thus formed will relax the inter-atomic forces exerted across the intersections between neighboring grains toward each other. But the forces are constrained by the adhesion of the substrate and then converted into volume strain energy. With further grain growth, the strain energy is reduced by the rearrangement of atoms and the elimination of grain boundaries. The relationship between the intrinsic stress and grain size can be expressed by:

$$\sigma = \frac{E_f \delta}{(1 - \nu_f)\theta} \quad , \tag{4}$$

where δ is the interaction potential across the grain and θ

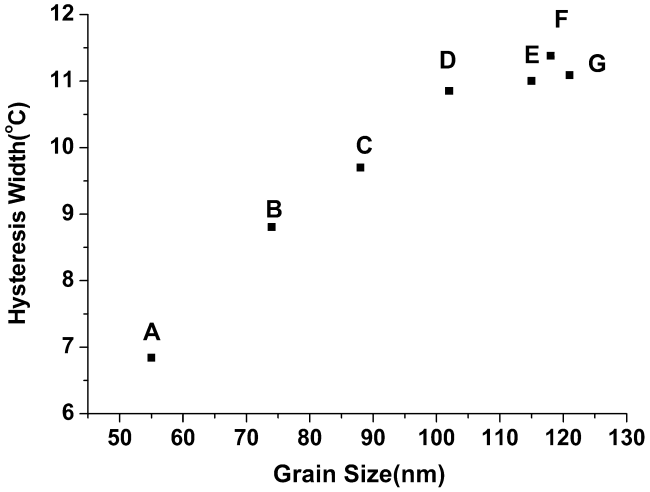

FIG. 7. The relationship between hysteresis width and grain size.

is the final grain size of the film. This equation shows that the tensile stress decreases with increasing grain sizes. However, the residual stress is found to decrease with the decrease of average grain sizes in some of our samples. The first reason of the opposite trend is poor crystalline structure in films of smaller grains. During processing at the same substrate temperature, smaller grain size means that low mobility of adatoms and nucleation dominates the early stage of film formation. Furthermore, strained and porous microstructures form easily. Experimental results of Martinez et al.[22] (who had investigated the effect of oxygen on stress in metallic films) showed that more oxygen in the metal and oxide of Cr (whose atomic size is close to vanadium) would induce more compressive stress superimposed on tensile stress and thus result in lower total tensile stress (even leading to compressive stress). Further internal oxidation through porous structure occurs in VO_2 films causing not only more compressive force but also locally inhomogeneous distribution of oxygen. On the other hand, the stress usually distributes inhomogeneously in polycrystalline films. At some portions, stress sustains (and it may be higher than) its local yield stress; while at other portions, it is lower than the yield stress. The film of smaller grain size usually has high possibility of poor crystallinity and more portions with stress that is larger than yield stress. In this circumstance, relaxation processes (such as movements of dislocations) occur more actively and residual stress becomes lower.

During the cooling of samples (the second step of stress formation), thermal stress arisen from film/substrate interaction causes movement of dislocations and adjustments of the residual stress. From the dislocation theory, grain boundaries that act as obstacles of dislocations, slip and lead to the pile-ups of dislocations behind grain boundaries. The number of dislocations in these pile-ups increases with grain size and applied stress. Furthermore, these pile-ups should produce stress concentration in the grains next to those containing pile-up. In larger grains, the stress multiplication in the next grain should be much larger; so that, beside intrinsic stress, a sample with larger grain sizes also has larger residual stress caused by external force. With superimposed intrinsic tensile stress and thermal stress from film/substrate interface, the film of smaller grain has smaller residual tensile stress.

The grain sizes of samples E, F, and G are almost the same, so the decrease of residual stress is caused by further crystallization during processing. In other words, samples F and G should have better crystallinity, so that the residual tensile stress is lower. Different crystallinity and residual stress also result in different optical-switching performance of VO_2 film.

The structure of VO_2 is monoclinic structure below Tt, while tetragonal rutile structure above Tt [as shown in Figs. 8(a) and 8(b)]. Central vanadium and six surrounding oxygen atoms form an octahedron structure at high temperature and a distorted octahedron structure at low temperature [as shown in Figs. 8(c) and 8(d)]. The former structure results in an insulator state of VO_2; and the later one, a metallic state. The distances, $d_{vo}s$, between central vanadium and surrounding oxygen atoms in distorted octahedron structure at insulator state before phase change are 0.176, 0.186, 0.187, 0.201, 0.203, and 0.205 nm, respectively, along different crystal axis. Yet, in the octahedron structure after phase change, it becomes 0.194 nm. The position adjustments of these seven atoms, especially contractions and expansions of bonds between vanadium and oxygen, are the primary structure changes during phase change, indicating that $d_{vo}s$ at low temperature dominate the Tt of VO_2. The stress exerted along c-axis influences Tt more than that along a- or b-axis.[17] As reported by Goodenough[1] and Lu et al.,[2] the angle between c- and a-axes is 123°. As shown in Fig. 8(a), c-axis, compared with a- and b-axes, is nearly parallel to z-axis that is the diagonal of distorted octahedron structure, also implying that this stress along c-axis mainly modifies the $d_{vo}s$ more than that along other axes. Besides, some $d_{vo}s$ are elongated and some are reduced during phase change; implying that, under the conservation of lattice volume, diagonal stress of distorted octahedral structure reduces the differences of $d_{vo}s$ before and after phase change. If each d_{vo} at low temperature is closer to that after phase transition, the threshold energy of phase change should become lower and Tt should be lower, too. The stress along the a- or b-axis may primarily adjust the relative position of these atoms, implying a higher driving force is required to move the atoms to an equilibrium state during cooling. Besides, during phase change, another intrinsic stress should form to overcome the barrier caused by the residual stress. Because atoms move only locally during phase change, the implication

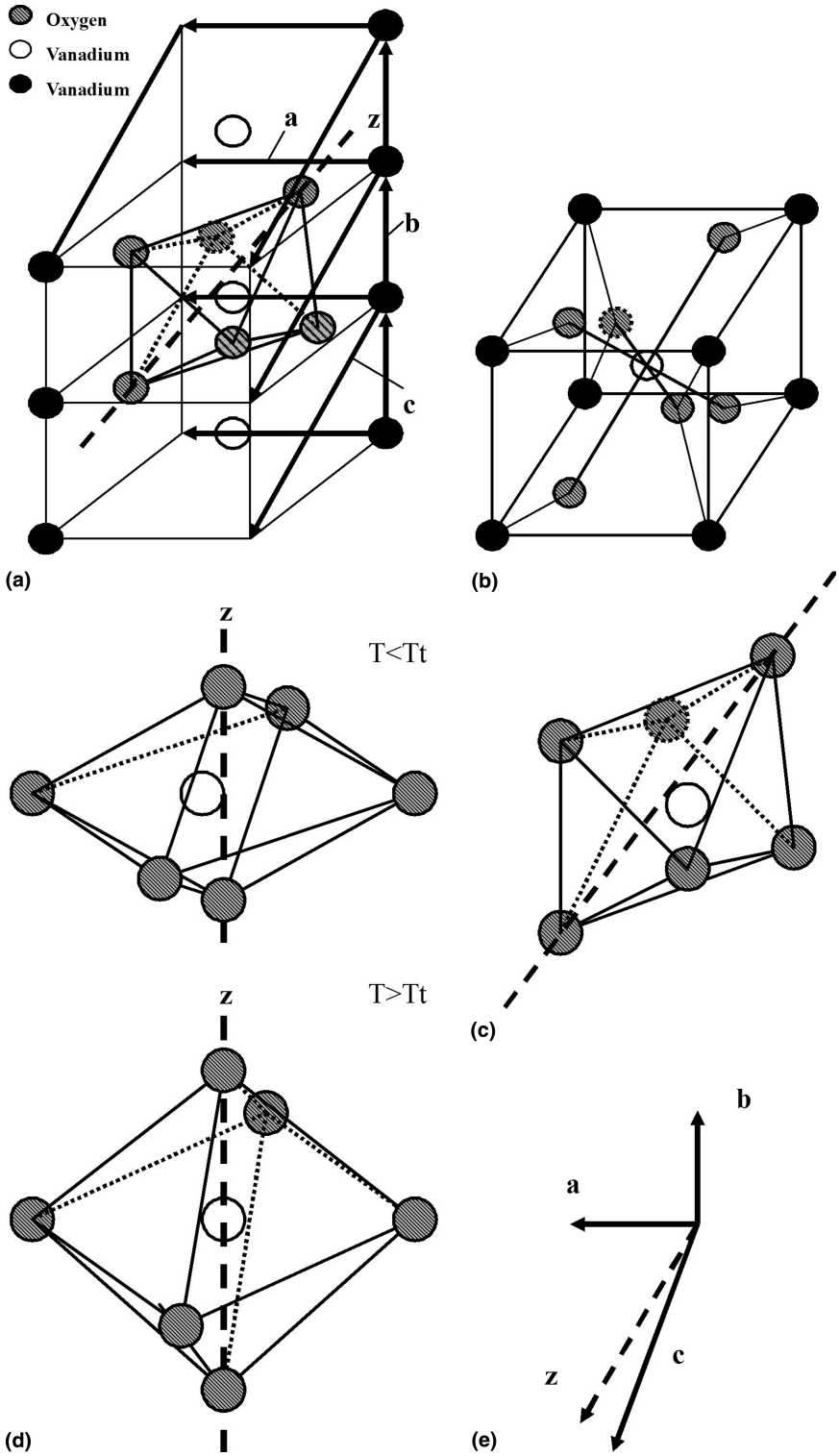

FIG. 8. (a) Monoclinic structure of VO_2 films below Tt (Tt); (b) tetragonal structure of VO_2 films above Tt (Tt); (c) distorted octahedron structure abstracted from monoclinic structure of VO_2; (d) change of octahedron structure before and after phase change; and (e) relative directions of a-, b-, c- and z-axes.

is that it is impossible to release residual stress simply by phase change. If the residual stress is large, this intrinsic stress, originated from thermal movement, should be large, to overcome the barrier of phase change. During cooling, a large Tt delay of phase change is also required to make the thin film return to the state of originally large residual stress. Therefore, a large hysteresis width forms under large residual stress.

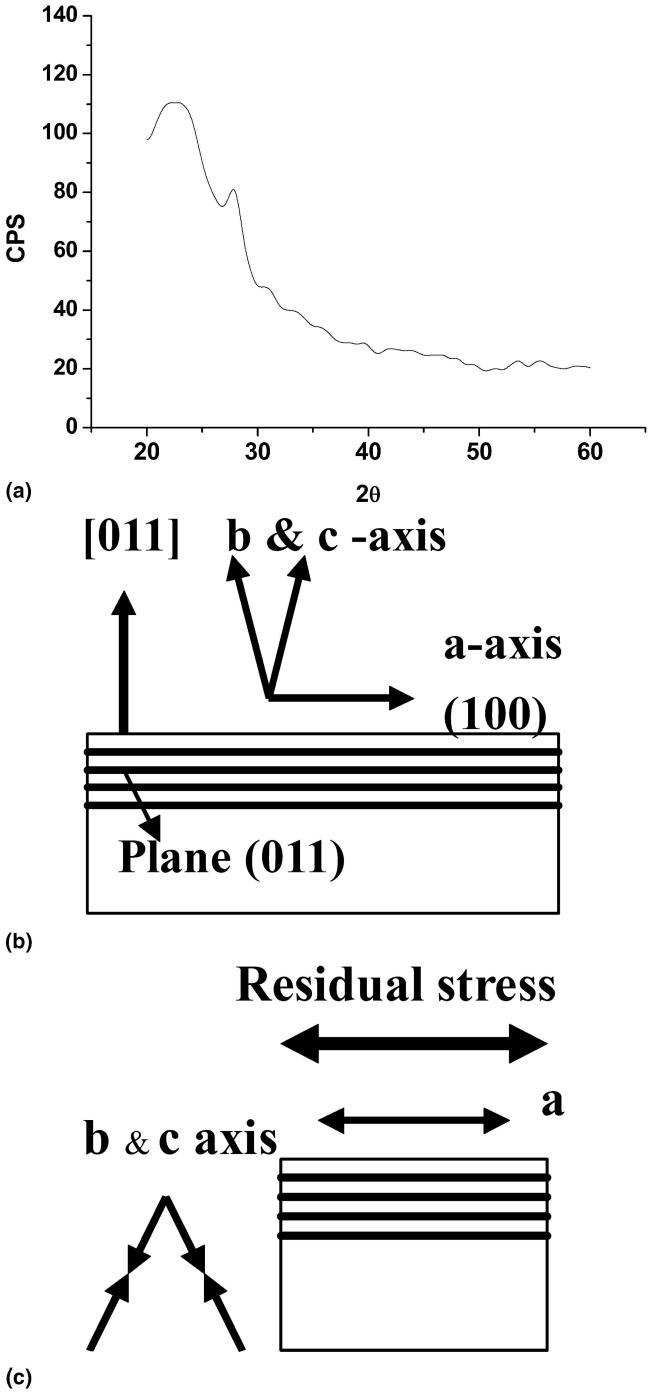

FIG. 9. (a) An XRD pattern of VO_2 by sputtering deposition; (b) indications of structure coordination, plane (011) and its normal direction; and (c) directions of the residual stress and deformations along a-, b- and c-axes. Under tensile residual stress, a axis is extended, thus b and c axes are both contracted.

From the θ–2θ scan of XRD, as shown in Fig. 9(a), the only peak at around 28° shows that the prepared films have preferred orientation [011], implying that plane (011) and a-axis are both parallel to the substrate surface. On the other hand, the b- and c-axis are nearly vertical to the film surface, as shown in Fig. 9(b). The bond length along a-axis is elongated by the residual stress, which is parallel to the film surface; on the contrary, bond lengths along b- and c-axes simultaneously contract for the conservation of total lattice volume, as shown in Fig. 9(c). The residual tensile stress, lying on the surface, directly results in the extension of bond length along a-axis and has larger effect to span the hysteresis. Therefore, the large hysteresis width forms especially in samples with larger grains, although the compression of bond length in c-axis is small. As shown in Fig. 7, the hysteresis width seems to reach a constant value as grain size increases. Although the residual stress seems to decrease in samples F and G, which show better crystallinity, the maintenance of hysteresis width implies a distortion limitation of a-axis. It is manifest that if the tensile stress is higher than a certain value in those thin films with larger grain size, the distortion along a-axis is restricted so that the hysteresis width is limited too. But with better crystallinity, the less residual stress properly causes less distortion along c-axis. Furthermore, the Tt becomes closer to the typical value in the films without residual stress. For films with smaller grain sizes, even though the residual stress inside is small, the intrinsic porous structure and internal oxidation contract bond lengths along b- and c-axes more than those in samples with larger grains, better crystalline structures, and less vertical compressive forces.

V. CONCLUSIONS

The relationship between as-deposited residual stress and transition temperatures (Tt) of VO_2 thin films was studied. The residual stress was quantitatively measured by x-ray diffractometry. The decrease in Tt of polycrystalline VO_2 films with (011) preferred orientation has been demonstrated to arise from the residual tensile stress that causes a contraction along c-axis of VO_2. It is also found that crystallinity of VO_2 films influences the residual stress under as-deposited state; and hence the Tt and hysteresis width. ESCA analysis on films with larger residual stress and poor crystallinity shows that the binding energy of core electrons becomes closer to the typical value of VO_2. This situation may arise from the relative positions of vanadium and oxygen atoms. From the theory of grain boundary formation, a secondary stress source arises most probably from the interactions between thermal stress and microstructure, which in turn is influenced by the inhomogeneity of VO_2 films. The secondary stress source is imposed to reduce residual tensile stress in the sample of smaller grain size. On the other hand, the inhomogeneity may also lead to further contraction of c-axis in the film with lower tensile stress, because the decrease of Tt has also been found. The tensile stress, parallel to the surface of the films, causes

the expansion of a-axis in films with [011] preferred orientation yet poor crystalline. Thus the width of transmittance loop was spanned. But for the films with better crystallinity, Tts are closer to the typical value as a result of lower distortion along c-axis under lower tensile stress. As the residual stress is higher than a critical value in the film with better crystallinity, the distortion along a-axis is constrained and the hysteresis width reaches a constant value. Further study is required to resolve the actual distorted structure of as-deposited VO_2 film and to identify the correlation between the phase-change behavior and relative positions of atoms at room temperature by high-resolution TEM analyses.

ACKNOWLEDGMENTS

This work was supported by the Ministry of Education of the Republic of China with the Academic Center of Excellence in "Photonics Science and Technology for Tera Era" under contract No. 89-E-FA06-1-4 and National Science Council of the Republic of China, under Grant No. NSC 91-2120-M007-001 and NSC 92-2120-M007-006. The stress measurement was done at the University of Illinois at Urbana-Champaign, performed in the Center for Microanalysis of Materials, the Fredrick Seitz Materials Research Laboratory. This portion of the work was supported by the U.S. Department of Energy under the project number DEFG02-96ER45439.

REFERENCES

1. J.B. Goodenough: The two components of the crystallographic transition in VO_2. *J. Solid State Chem.* **3,** 490 (1971).
2. S. Lu, L. Hou, and F. Gan: Structure and optical property changes of sol-gel derived VO_2 thin films. *Adv. Mater.* **9,** 244 (1997).
3. Y. Shigesato, M. Enomoto, and H. Odaka: Thermochromic VO_2 films deposited by RF magnetron sputtering using V_2O_3 or V_2O_5 targets. *Jpn. J. Appl. Phys.* **39,** 6016 (2000).
4. M.G. Krishna, Y. Debauge, and A.K. Bhattacharya: X-ray photoelectron spectroscopy and spectral transmittance study of stoichiometry in sputtered vanadium oxide films. *Thin Solid Films* **312,** 116 (1998).
5. C.H. Griffiths and H.K. Eastwood: Influence of stoichiometry on the metal-semiconductor transition in vanadium dioxide. *J. Appl. Phys.* **45,** 2201 (1974).
6. M. Fukuma, S. Zembutsu, and S. Miyazawa: Preparation of VO_2 thin film and its direct optical bit recording characteristics. *Appl. Opt.* **22,** 265 (1983).
7. G.A. Nyberg and R.A. Buhrman: Preparation and optical properties of reactively evaporated VO_2 thin films. *J. Vac. Sci. Technol. A* **2,** 301 (1984).
8. J.M. Gregg and R.M. Bowman: Effect of applied strain on the resistance of VO_2 thin films. *Appl. Phys. Lett.* **71,** 3649 (1997).
9. C. Zheng, X. Zhang, and J. Zhang: Preparation and Characterization of VO_2 Nanopowders. *J. Solid State Chem.* **156,** 274 (2001).
10. G. Guzman, F. Beteille, R. Morineau, and J. Livage: Electrical switching in VO_2 sol-gel films. *J. Mater. Chem.* **6,** 505 (1996).
11. S. Lu, L. Hou, and F. Gan: Surface analysis and phase transition of gel-derived VO_2 thin films. *Thin Solid Films* **353,** 40 (1999).
12. S. Lu, L. Hou, and F. Gan: Preparation and optical properties of phase-change VO_2 thin films. *J. Mater. Sci.* **28,** 2177 (1993).
13. D.D. Eden: Optical properties of VO_2 thin films. *Optical Processing Systems* **185,** 97 (1978).
14. F. Guinneton, L. Sauques, J.C. Valmalette, F. Cros, and J.R. Gavarri: Comparative study between nanocrystalline powder and thin film of vanadium dioxide VO_2: Electrical and infrared properties. *J. Phys. Chem. Solids* **62,** 1229 (2001).
15. Y. Muraoka, Y. Ueda, and Z. Hiroi: Large modification of the metal-insulator transition temperature in strained VO_2 films grown on TiO_2 substrates. *J. Phys. Chem. Solids* **63,** 965 (2002).
16. F.C. Case: Influence of ion beam parameters on the electrical and optical properties of ion-assisted reactively evaporated vanadium dioxide films. *J. Vac. Sci. Technol. A* **5,** 1762 (1987).
17. C.H. Ma, J.H. Huang, and Haydn Chen: Residual stress measurement in textured thin film by grazing-incidence x-ray diffraction. *Thin Solid Films* **418,** 73 (2002).
18. G.A. Sawatzky and D. Post: X-ray photoelectron and Auger spectroscopy study of some vanadium oxides. *Phys. Rev. B* **20,** 1546 (1979).
19. T. Christmann, B. Felde, W. Niessner, D. Schalch, and A. Scharmann: Thermochromic VO_2 thin films studied by photoelectron spectroscopy. *Thin Solid Films* **287,** 134 (1996).
20. J.D. Finegan and R.W. Hoffman: Stress anisotropy in evaporated iron films. *J. Appl. Phys.* **30,** 597 (1959).
21. F.A. Doljack and R.W. Hoffman: The origins of stress in thin nickel films. *Thin Solid Films* **12,** 71 (1972).
22. H.P. Martinz and R. Abermann: Interaction of O_2, CO, H_2O, H_2 and N_2 with thin chromium films studied by internal stress measurements. *Thin Solid Films* **89,** 133 (1982).